Theoretical Study in $[C_2H_4–Tl]^+$ and $[C_2H_2–Tl]^+$ Complexes

FERNANDO MENDIZABAL,[1] CLAUDIO OLEA-AZAR[2]

[1]*Departamento de Química, Facultad de Ciencias, Universidad de Chile, Casilla 653, Santiago, Chile*

[2]*Departamento de Química Inorgánica y Analítica, Facultad de Ciencias Químicas y Farmacéuticas, Universidad de Chile, Casilla 233, Santiago 1, Chile*

ABSTRACT: We studied the attraction between $[C_2H_n]$ and Tl(I) in the hypothetical $[C_2H_n–Tl]^+$ complexes (n = 2,4) using ab initio methodology. We found that the changes around the equilibrium distance C–Tl and in the interaction energies are sensitive to the electron correlation potential. We evaluated these effects using several levels of theory, including Hartree–Fock (HF), second-order Møller–Plesset (MP2), MP4, coupled cluster singles and doubles CCSD(T), and local density approximation augmented by nonlocal corrections for exchange and correlation due to Becke and Perdew (LDA/BP). The obtained interaction energies differences at the equilibrium distance R_e (C–Tl) range from 33 and 46 kJ/mol at the different levels used. These results indicate that the interaction between olefinic systems and Tl(I) are a real minimum on the potential energy surfaces (PES). We can predict that these new complexes are viable for synthesizing. At long distances, the behavior of the $[C_2H_n]–Tl^+$ interaction may be related mainly to charge-induced dipole and dispersion terms, both involving the individual properties of the olefinic π-system and thallium ion. However, the charge-induced dipole term (R^{-4}) is found as the principal contribution in the stability at long and short distances.

Key words: Tl(I); olefinic; quasi-relativistic effects

Correspondence to: F. Mendizabal; e-mail: hagua@uchile.cl

Contract grant sponsor: FONDECYT.
Contract grant sponsor: CONICYT-Chile.
Contract grant number: 1020141.
Contract grant sponsor: Millennium Nucleus for Applied Quantum Mechanics and Computational Chemistry (MIDEPLAN).
Contract grant number: P02-004-F.

Introduction

Closed-shell interactions range from extremely weak van der Waals forces to metallophilic and extremely strong d^{10}–s^2 or s^2–s^2 interactions [1, 2]. For example, reports can be found in the literature for diatomic systems with d^{10}–s^2 strong closed-shell interactions such as $AuHg^+$ and $AuXe^+$ with interaction energies of 179 and 87 kJ/mol, respectively [3–5]. Also, in the $[Pt(PH_3)_3]$–Tl^+ complex, the interaction energy Pt(0)–Tl(I) is 205 kJ/mol at the CCSD(T) level, corresponding to the strong closed shell [6]. In general, for these systems, two complementary forces have been identified: charge-induced dipole (cid) and dispersion (disp) interactions [7]. The largest contribution to the total energy is due to the charge-induced dipole interaction term; nevertheless, the dispersion effects acquire significance near the equilibrium bond lengths. This is obtained when some from the subsystems presents an electronic configuration of the type s^2, the one that is inert.

In contrast, one could think about a closed-shell organometallic hypothetical complex between an olefinic π-system (L) and transition metal (M) s^2 with the objective that in such systems the forces of charge-induced dipole and dispersion prevail as an interaction of the van der Waals type. The $[Pt(PH_3)_3]$ complex [Pt(0)] or Au(I) (d^{10}) can be compared with C_2H_4 (π^2) and C_2H_2 (π^4) with respect to an underoxidation state and high electronic density. If the transition metal is a thallium(I) ion, s^2, the formation of the complex is avoided by the Dewar–Chatt–Duncanson model (synergistic combination of σ-donor and π-acceptor interaction between the metal and the olefinic π-system, back-donation) [8, 9]. The latter occurs when the cations used are coinage transition metals (Cu(I), Ag(I), and Au(I)) [10–12].

There are no reported complexes of the $[L–Tl]^+$ type at the theoretical and experimental levels with the olefinic π-system neutral. In the literature, complexes of the Cp–Tl (Cp: pentamethylcyclopentadienyl and pentabenzylcyclopentadienyl anions) type are described, demonstrating an ionic interaction [13, 14].

In the present work, we detail a theoretical study of the formation of the $[C_2H_4–Tl]^+$ (C_{2v}) and $[C_2H_2–Tl]^+$ (C_2) complexes (Fig. 1) as intermolecular interaction models π^2–s^2 and π^4–s^2 in organometallic systems, comparing the C–Tl(I) distances and estimating the strength of these interactions at the Hartree–Fock (HF), second-order Møller–Plesset (MP2), MP4, coupled cluster singles and doubles CCSD(T), and local density approximation augmented by nonlocal corrections for exchange and correlation due to Becke and Perdew (LDA/BP). We report the structures and stability of these compounds and predict the most promising targets for synthetic work. Also, to estimate the nature of the intermolecular interactions, we have included two simple expressions: charge-induced dipole and dispersion, calculated from the individual properties of C_2H_4 (π^2), C_2H_2 (π^4), and Tl(I) at the MP2 level [4].

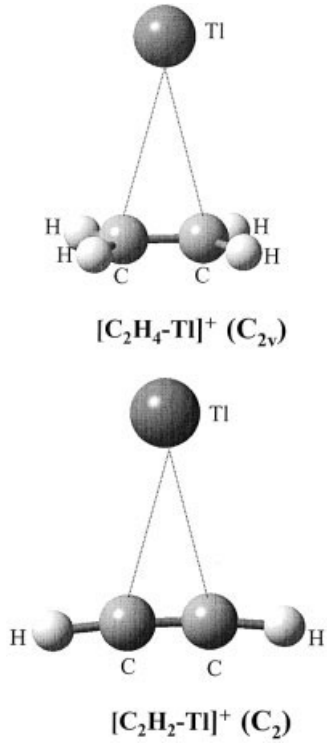

FIGURE 1. Models of $[C_2H_4–Tl]^+$ and $[C_2H_2–Tl]^+$ complexes.

Computational Details

The calculations were carried out with Gaussian 98 [15]. For the heavy element Tl, we used the Stuttgart quasi-relativistic pseudo-potential (PP) 21-VE [16]. Two *f*-type polarization functions were added to Tl (α_f = 1.0, 0.36) [17]. Also, the C atom was treated with PP, using the double-zeta basis set and adding one *d*-type polarization function [18]. For hydrogen, a valence-double-zeta basis set with *p*-polarization functions was used [19].

TABLE I

Geometries (pm and deg), interaction energies (V(R_e), kJ/mol), and force constant (F) C–Tl (Nm^{-1}) for $[C_2H_4–Tl]^+$ using RECP for HF, MP2, MP4, and CCSD(T); the non(N)- and quasi-relativistic (QR) approach for LDA/BP.

	HF	MP2	MP4	CCSD(T)	LDA/BP(QR)	LDA/BP(NR)
Tl–C	338.9	307.9	312.2	315.2	294.6	340.6
C–C	132.7	134.7	135.1	135.2	134.0	134.0
C–H	108.4	109.4	109.6	109.7	109.0	109.0
CCH°	121.6	121.3	121.4	121.4	121.6	121.5
HCCH° [a]	175.0	174.9	174.9	175.3	173.8	180.0
V(R_e)	−33.1	−46.4	−41.4	−38.9	−44.1	−37.3
F	2.43	4.09	3.55	3.31	3.75	2.89

[a] As compared with 180° in ethylene free.

Fully optimized geometries were determined by employing the HF, MP2, MP4, and CCSD(T) methods. Although the computational methodologies do not consider spin-orbit interactions, the complexes under investigation are a closed-shell singlet and should therefore have only minor importance. The counterpoise correction for the basis-set superposition error (BSSE) was used for the calculated interaction energies. The vibrational frequencies were computed in both models, using the different methods, with the objective of having thoroughly optimized geometry without imaginary frequencies.

In contrast, we also have optimized geometries employing LDA/BP with the ADF suite of programs [20]. Inner-shell electrons ([He] for C and [Xe]$4f^{14}$ for Tl) were treated in the frozen-core approximation [21–23], and the valence orbitals were expanded as lineal combinations of Slater-type orbital (STO) basis functions. Triple-zeta plus polarization basis sets were used for thallium, carbon, and hydrogen, respectively. The nonrelativistic (NR) and quasi-relativistic (QR) treatment were employed with analytic gradient techniques. The objective with this methodology is to quantify approximately the relativistic effect of the ion Tl (I) in the hypothetical complexes.

Results and Discussion

Tables I and II summarize the principal geometric parameters, interaction energies and the force constants C–Tl obtained for the optimized geometries at several theoretical levels. In this section, we will discuss about the geometries and the energies of the $C_2H_4\cdots Tl^+$ and $C_2H_2\cdots Tl^+$ interaction in the complexes proposed. To determine the scalar relativistic effect in the complexes, the DFT(LDA/BP) methodology was applied at the NR and QR levels. For the complexes, the frequencies have been calculated at the different levels (Tables III and IV). Also, the natural bond orbital (NBO) analysis is

TABLE II

Geometries (pm and deg), interaction energies (V(R_e), KJ/mol), and force constant (F) C–Tl (Nm^{-1}) for $[C_2H_2–Tl]^+$ using RECP for HF, MP2, MP4, and CCSD(T); the non(N)- and quasi-relativistic (QR) approach for LDA/BP.

	HF	MP2	MP4	CCSD(T)	LDA/BP(QR)	LDA/BP(NR)
Tl–C	323.6	299.9	303.7	308.3	307.9	337.3
C–C	119.3	122.7	122.9	122.6	120.0	120.0
C–H	106.6	107.8	107.9	108.0	107.0	107.0
CCH°	176.2	175.7	175.5	175.6	175.3	176.6
HCCH° [a]	0.05	1.13	1.13	0.50	18.76	11.73
V(R_e)	−31.3	−44.3	−41.3	−38.7	−41.8	−32.6
F	3.49	6.53	5.77	5.13	5.72	3.65

[a] As compared with 0° in acetylene free.

TABLE III

Calculated harmonic frequencies (cm^{-1}) for $[C_2H_4–Tl]^+$ (C_{2v}).

Mode	HF	MP2	MP4	CCSD(T)
$1b_2$	91	84	78	80
$1a_1$	98	116	108	104
$1b_1$	222	208	203	201
$2b_1$	888	834	827	826
$2b_2$	1097	966	945	940
$2a_1$	1118	1030	1010	1004
$1a_2$	1138	1075	1053	1044
$2a_2$	1335	1249	1242	1241
$3a_1$	1465	1382	1368	1365
$2b_2$	1573	1479	1473	1472
$4a_1$	1806	1678	1667	1668
$3b_2$	3298	3192	3164	3155
$4a_1$	3314	3204	3177	3169
$3a_2$	3379	3287	3254	3243
$3b_1$	3402	3307	3274	3264

given in Table V. Finally, the nature of the intermolecular interactions will be studied as simple inductive and dispersion expressions obtained for the individual properties of the olefinic π-system (ethylene and acetylene) and the thallium ion (Table VI).

SHORT-DISTANCE BEHAVIOR

The results of our calculations (see Tables I and II) support the original idea proposed that the $[C_2H_n–Tl]^+$ systems show weak closed-shell interactions of the van der Waals type. Concerning the C–Tl distance and the interaction energy, it is clear

TABLE IV

Calculated harmonic frequencies (cm^{-1} for $[C_2H_2–Tl]^+$ (C_2).

Mode	HF	MP2	MP4	CCSD(T)
1a	90	126	118	111
2b	140	136	132	131
2a	767	573	520	518
2b	784	618	568	565
3b	871	767	749	745
3a	903	809	793	787
4a	2221	1972	1960	1990
4b	3548	3423	3398	3390
5a	3662	3511	3488	3484

TABLE V

NBO analysis of the MP2 density for $[C_2H_4–Tl]^+$ and $[C_2H_2–Tl]^+$.

System	Atom	Natural	Natural electron configuration
$[C_2H_4–Tl]^+$	Tl	0.9512	$6s^{1.94}6p^{0.11}5f^{0.10}6d^{0.03}7p^{0.01}$
	C	−0.4110	$2s^{1.08}2p^{3.28}3s^{0.01}3p^{0.02}3d^{0.02}$
	H	0.2175	$1s^{0.78}$
$[C_2H_4]$	C	−0.3715	$2s^{1.06}2p^{3.27}3p^{0.02}3d^{0.02}$
	H	0.1858	$1s^{0.81}$
Tl(I)	Tl	1.0000	$5d^{10.0}6s^{2.00}6p^{0.00}$
$[C_2H_2–Tl]^+$	Tl	0.9609	$6s^{1.94}6p^{0.11}5f^{0.10}6d^{0.03}7p^{0.01}$
	C	−0.2448	$2s^{1.04}2p^{3.17}3s^{0.01}3p^{0.01}3d^{0.02}$
	H	0.2638	$1s^{0.73}$
$[C_2H_2]$	C	−0.2226	$2s^{1.02}2p^{3.17}3s^{0.01}3p^{0.01}3d^{0.02}$
	H	0.2226	$1s^{0.77}$
Tl(I)	Tl	1.0000	$5d^{10.0}6s^{2.00}6p^{0.00}$

that the electronic correlation effects play an important role in the stability of both systems. The C–Tl distances obtained with all methods are close to the van der Waals type (from 294 pm to 338 pm). However, the distance obtained with the MP2 and LDA/BP(QR) methods are the shortest. It is worth noting that both approximations overestimate the weak interactions [24, 25]. The density functional theory (DFT) results are less appropriate for the present interaction. The distances obtained in this work indicate that the C···Tl contact is a weak closed-shell interaction on the $C_2H_4\cdots Tl^+$ and $C_2H_2\cdots Tl^+$ complexes. Also, the C–Tl force constants (F) calculated in the complexes are indicative of a weak interaction.

Another manifestation of a weak interaction in the complexes is the dihedral angle HCCH°. This angle shows low deviation compared with the ethylene and acetylene free. Different behavior has been observed theoretically [10–12] when the presence of a M^+ cation (M = Au, Ag, Cu) on the ethylene ligand generates the rehybridization of the carbon centers from sp^2 toward sp^3, resulting in a partial pyramidalization of the two carbons. The

TABLE VI

Finite field calculations (a.u.) of electric properties of C_2H_4, C_2H_2, and Tl(I) at MP2 level.

Properties	C_2H_4	C_2H_2	Tl(I)
Polarizability (α)	20.3757	14.9923	18.8141
First ionization potential (IP_1)	0.3674	0.3969	0.6749

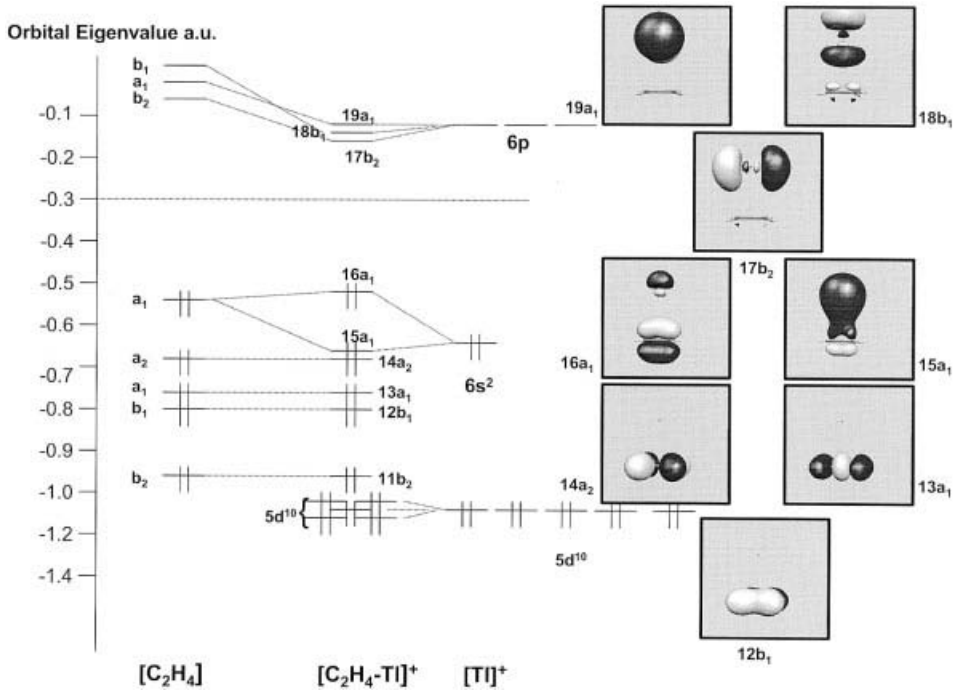

FIGURE 2. Interaction diagram obtained for the frontier molecular orbitals for $[C_2H_4]$ (C_{2v}) and Tl^+ fragments.

dihedral angle HCCH° shows strong deviation. This was explained through a synergistic combination of σ-donor and π-acceptor interaction between the metal and the olefinic $\pi\pi$-system, commonly designated back-donation [8, 9].

The magnitude of the interaction energies obtained varies according to the method used between 33.1 kJ/mol (HF) and 46.4 kJ/mol (MP2) in $[C_2H_4–Tl]^+$, and 31.3 kJ/mol (HF) and 44.3 kJ/mol in $[C_2H_2–Tl]^+$. Such magnitudes are generally associated with weak interactions. However, this might be indicative of an orbital stabilization due to the formation of stable adducts between the olefinic π-system (ethylene and acetylene) and the thallium ion. This is because the complexes are already stabilized at the HF level, as can be appreciated in Tables I and II.

To obtain further insight into this stabilization, we have depicted in Figures 2 and 3 an interaction diagram for the frontier molecular orbitals of both fragments olefinic π-system (ethylene and acetylene) and Tl^+ ion at the MP2 level. In Figures 2 and 3, the left and right side correspond to the frontier levels of the olefinic π-system and thallium ion, respectively. The center of the diagram corresponds to the molecular orbitals for the $[C_2H_4–Tl]^+$ (C_{2v}) and $[C_2H_2–Tl]^+$ (C_2) complexes, respectively. Two orbitals show a strong interaction: $16a_1$ and $15a_1$ in $[C_2H_4–Tl]^+$ and 15a and 13a in $[C_2H_2–Tl]^+$, whereas the molecular orbitals remain without changes (except the LUMO levels). Both group of orbitals generate the bonding ($15a_1$ and 13a) and antibonding ($16a_1$ and 15a) sigma levels from olefinic π occupied (ethylene and acetylene) and $6s^2$ (Tl), respectively. These two molecular orbitals are doubly occupied. These results clearly indicate a net effect of no bonding through the orbital interactions.

The scalar relativistic effect in the interaction of the complexes through the QR and NR is studied at the LDA Becke–Perdew (BP) level. The results displayed in Tables I and II show that the interaction energies in $[C_2H_4–Tl]^+$ and $[C_2H_2–Tl]^+$ complexes are stabilized by 15% and 22%, respectively, on going from NR to QR LDA/BP. Thus, the relativistic effect is present and contributes to increase the interactions of Tl^+ with ethylene and acetylene.

We have calculated the frequencies of the complexes at different levels (see Tables III and IV). We note that the harmonic frequencies are in reasonable agreement with each other. Thus, the interaction between Tl^+ and olefinic systems is a real minimum on the potential energy surfaces (PES). It is possible to observe oscillations in this property according to the calculation method used. Within

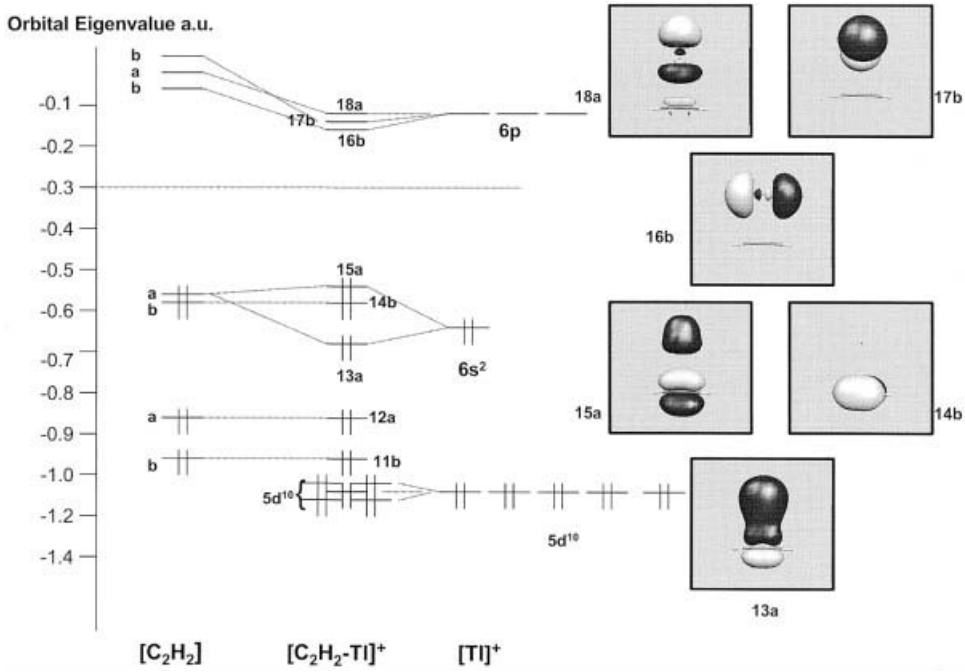

FIGURE 3. Interaction diagram obtained for the frontier molecular orbitals for $[C_2H_2]$ (C_2) and Tl^+ fragments.

the objectives of the study, an important frequency in both complexes is the first ($1b_2$ in $[C_2H_4–Tl]^+$ and $1a$ in $[C_2H_2–Tl]^+$). This frequency corresponds to stretching between Tl^+ and the two carbon atoms in ethylene and acetylene. The low frequencies associated with the Tl^+–(C_2H_4) and Tl^+–(C_2H_2) motions indicate a weak interaction.

The NBO [24] population analysis for the complexes is shown in Table V. This analysis is based on the MP2 density. In Table V, a small charge transfer from the olefinic π-system (ethylene and acetylene) toward the thallium ion can be observed in the complexes under study. The charge on the Tl ion is due mainly to a charge transfer from the hydrogen atoms. The carbons show no variability in charge. This could suggest a weak interaction between the carbons and the Tl ion. The gross population per atom shell shows that for the 6*p* orbital (0.11e) belonging to thallium takes advantage of this charge transfer by increasing its occupation. This could suggest a possible orbital interaction among both fragments. The charge of the 6*s* orbital, on the contrary, does not change, maintaining its inert character.

LONG-DISTANCE BEHAVIOR

The HF and MP2 results for the long-distance attraction between the olefinic π-system (ethylene and acetylene) and Tl^+ are shown in Figures 4 and 5. Very similar results have been obtained with the MP4 and CCSD (T) methods (not shown in the present study). Energy minima occur at R_e (see Tables I and II). At the equilibrium distance R_e (C–Tl), the differences in energy between the HF and MP2 levels corresponds to the electronic correlation effects. At long-range distances, it can be noted that the HF term is prevailing. We have used Eq. (1) to describe the terms involved in the limit of large distances. This equation includes the charge-induced dipole (cid) and the dispersion (disp) terms, which can be used to understand the predominant mechanism of bonding:

$$E = Ecid + Edisp = -1/2\,\frac{\alpha^{[C2Hn]}q^2}{R^4} - 3/2\,\frac{\alpha^{[C2Hn]}\alpha^{Tl}}{R^6}\left[\frac{PI^{[C2Hn]}PI^{Tl}}{PI^{[C2Hn]}+PI^{Tl}}\right].$$

Table VI lists the polarizability (α) and ionization potentials (IP) used for olefinic π-system (ethylene and acetylene) and Tl(I) obtained at the MP2 level. It is evident from the greater slope observed in the charged-induced dipole interaction curve that this term predominates over the dispersion force. This

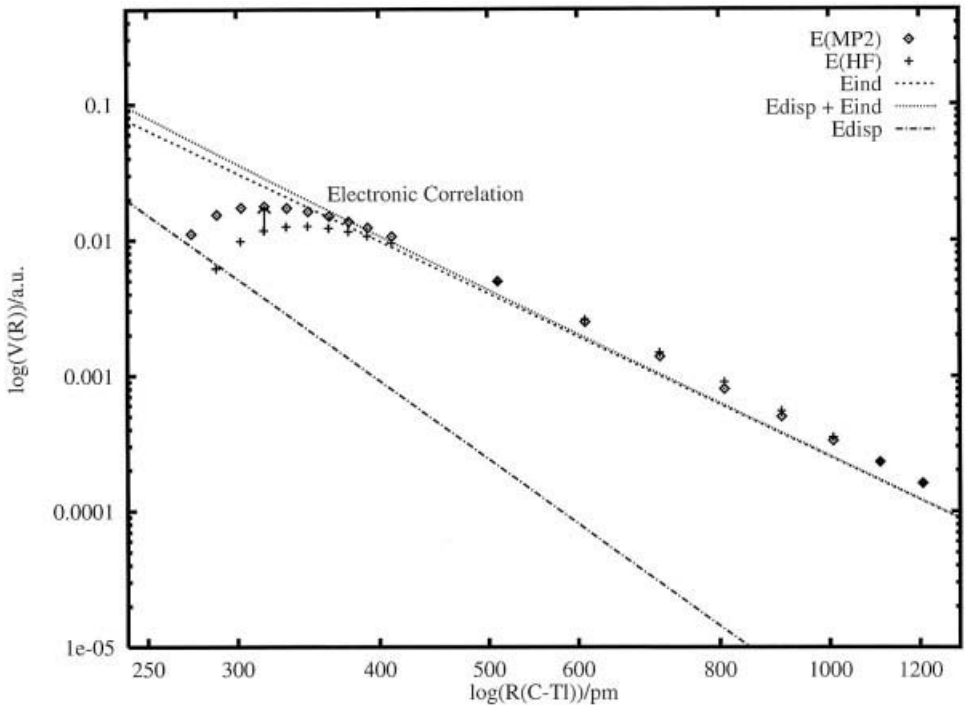

FIGURE 4. Calculated interaction energies of the $[C_2H_4–Tl]^+$ model at the HF and MP2 levels.

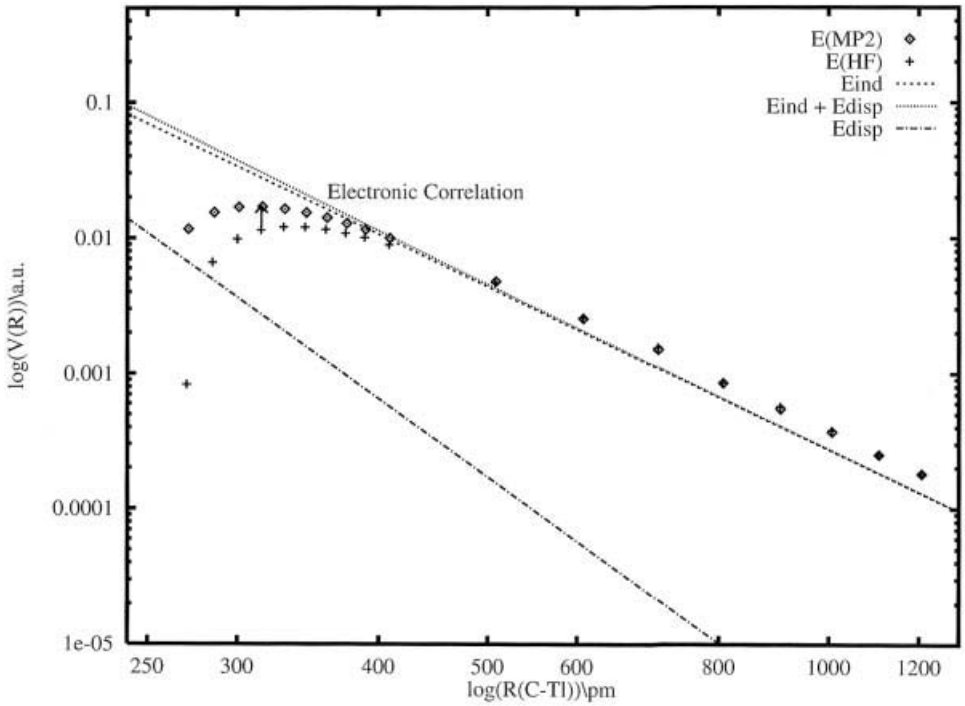

FIGURE 5. Calculated interaction energies of the $[C_2H_2–Tl]^+$ model at the HF and MP2 levels.

may shed light on why C–Tl bonds at the HF level. At the MP2 level in the C–Tl equilibrium distance, the contribution of the charge-induced dipole term is prevailing, though the dispersion term is not negligible. For $[C_2H_4–Tl]^+$ and $[C_2H_4–Tl]^+$ systems the contribution of the charge-induced dipole term are 72% and 70%, respectively. While the dispersion term are 28% and 30%, respectively.

Conclusions

The calculated interaction energies of the $[C_2H_n–Tl]^+$ complexes could be explained in terms of long-range polarization and dispersion interactions, in which the attractive term is dominant in the potential coming from the polarization of ethylene and acetylene by Tl^+. The largest contribution energy is the charge-induced dipole interaction of Eq. (1), but dispersion effects are significant near the equilibrium bond length. The complexes studied in the present work show R^{-4} behavior at large distances. Moreover, the NBO analysis showed a small charge transfer from the olefinic systems toward the thallium ion, but this cannot be understood as a classic dative interaction. This is confirmed by an orbital analysis, which shows that a formal bond through an orbital interaction does not exist. If scalar relativistic effects are omitted, the attraction $V(R_e)$ decreases in 15% and 22% by $[C_2H_4–Tl]^+$ and $[C_2H_2–Tl]^+$, respectively.

References

1. Pyykkö, P. Chem Rev 1997, 97, 597.
2. Luo, F.; Mcbane, G. C.; Kim, G.-S.; Giese, C. F.; Gentry, W. R. J Chem Phys 1993, 98, 3564.
3. Wesendrup, R.; Schwerdtfeger, P. Angew Chem Int Ed 2000, 39, 907.
4. Schröder, D.; Schwarz, H.; Hrusák, J.; Pyykkö, P. Inorg Chem 1998, 37, 624.
5. Pyykkö, P. J Am Chem Soc 1995, 117, 2067.
6. Mendizabal, F.; Zapata-Torres, G.; Olea-Azar, C. Chem Phys Lett 2005, 412, 477.
7. Read, J. P.; Buckingham, A. D. J Am Chem Soc 1997, 119, 9010.
8. Dewar, M. J. S. Bull Soc Chim Fr 1951, C79, 18.
9. Chatt, J.; Duncanson, L. A. J Chem Soc 1953, 2939.
10. Ziegler, T.; Rauk, A.; Inorg Chem 1979, 18, 1558.
11. Hrusák, J.; Hertwig, R. H.; Schröder, D.; Schwerdtfeger, P.; Koch, W.; Schwarz, H. Organometallics 1995, 14, 1284.
12. Hertwig, R. H.; Koch, W.; Schröder, D.; Schwarz, H.; Hrusák, J.; Schwerdtfeger, P. J Phys Chem 1996, 100, 12253.
13. Beswick, M. A.; Palmer, J. S.; Wright, D. S. Chem Soc Rev 1998, 27, 225.
14. Ghosh, P.; Rheingold, A. L.; Parkin, G. Inorg Chem 1999, 38, 5464.
15. Frisch, M. J.; Trucks, G. W.; Schlegel, H. B.; Scuseria, G. E.; Robb, M. A.; Cheeseman, J. R.; Zakrzewski, V. G.; Montgomery Jr., J. A.; Stratmann, R. E.; Burant, J. C.; Dapprich, S.; Millam, J. M.; Daniels, A. D.; Kudin, K. N.; Strain, M. C.; Farkas, Ö.; Tomasi, J.; Barone, V.; Cossi, M.; Cammi, R.; Mennucci, B.; Pomelli, C.; Adamo, C.; Clifford, S.; Ochterski, J.; Petersson, G. A.; Ayala, P. Y.; Cui, Q.; Morokuma, K.; Salvador, P.; Dannenberg, J. J.; Malick, D. K.; Rabuck, A. D.; Raghavachari, K.; Foresman, J. B.; Cioslowski, J.; Ortiz, J. V.; Baboul, A. G.; Stefanov, B. B.; Liu, G.; Liashenko, A.; Piskorz, P.; Komáromi, I.; Gomperts, R.; Martin, R. L.; Fox, D. J.; Keith, T.; Al-Laham, M. A.; Peng, C. Y.; Nanayakkara, A.; Challacombe, M.; Gill, P. M. W.; Johnson, B.; Chen, W.; Wong, M. W.; Andres, J. L.; Gonzalez, C.; Head-Gordon, M.; Replogle, E. S.; Pople, J. A. Gaussian 98: Pittsburgh, PA, 1998.
16. (a) Andrae, D.; Haeussermann, U.; Dolg, M.; Stoll, H.; Preuss, H. Theor Chim Acta 1990, 77, 12; (b) Leininger, T.; Berning, A.; Nicklass, A.; Stoll, H.; Wener, H. J.; Flad, H. J Chem Phys 1997, 217, 19.
17. Pyykkö, P.; Straka, M.; Tamm, T. Phys Chem Chem Phys 1999, 1, 3441.
18. Bergner, A.; Dolg, M.; Küchle, W.; Stoll, H.; Preuss, H. Mol Phys 1993, 80, 1431.
19. Huzinaga, S. J Chem Phys 1965, 42, 1293.
20. ADF; version 2.3: (a) Baerends, E. J.; Ellis, D. E. Chem Phys 1973, 2, 71; (b) te Velde, G.; Baerends, E. J. J Comp Phys 1992, 99, 84.
21. Snijders, J. G.; Baerends, E. J. Mol Phys 1977, 33, 1651.
22. Ziegler, T.; Rauk, A. Theor Chim Acta 1977, 46, 1.
23. Kiaura, K.; Morukuma, K. Int J Quantum Chem 1976, 10, 325.
24. Pyykkö, P.; Mendizabal, F. Inorg Chem 1998, 37, 3018.
25. Mendizabal, F.; Zapata-Torres, G.; Olea-Azar, C. Chem Phys Lett 2003, 382, 92.
26. Carpenter, J. E.; Weinhold, F. J Mol Struct 1988, 169, 41.